

# Scaling properties of background- and chiral-magnetically-driven charge separation: evidence for detection of the chiral magnetic effect in heavy ion collisions

Roy Lacey<sup>1,\*</sup>

<sup>1</sup>Depts. of Chemistry & Physics, Stony Brook University, Stony Brook, New York 11794, USA

**Abstract.** The scaling properties of the  $R_{\Psi_2}(\Delta S)$  correlator and the  $\Delta\gamma$  correlator are used to investigate a possible chiral-magnetically-driven (CME) charge separation in  $p$ +Au,  $d$ +Au, Ru+Ru, Zr+Zr, and Au+Au collisions at  $\sqrt{s_{\text{NN}}} = 200$  GeV, and in  $p$ +Pb ( $\sqrt{s_{\text{NN}}} = 5.02$  TeV) and Pb+Pb collisions at  $\sqrt{s_{\text{NN}}} = 5.02$  and 2.76 TeV. The results for  $p$ +Au,  $d$ +Au,  $p$ +Pb, and Pb+Pb collisions, show the  $1/N_{\text{ch}}$  scaling for background-driven charge separation. However, the results for Au+Au, Ru+Ru, and Zr+Zr collisions show scaling violations which indicate a CME contribution in the presence of a large background. In mid-central collisions, the CME accounts for approximately 27% of the signal + background in Au+Au and roughly a factor of two smaller for Ru+Ru and Zr+Zr, which show similar magnitudes.

Metastable domains of gluon fields with non-trivial topological configurations can form in the magnetized chiral relativistic quark-gluon plasma (QGP) [1] produced in collisions at RHIC and the LHC. The colliding ions generate the magnetic field ( $\vec{B}$ ) at early times [2]. The interaction of chiral quarks with the gluon fields can drive a chiral imbalance resulting in an electric current  $\vec{J}_V = \frac{N_c e \vec{B}}{2\pi^2} \mu_A$ , along the  $\vec{B}$ -field, i.e., roughly perpendicular to the reaction plane;  $N_c$  is the color factor, and  $\mu_A$  is the axial chemical potential that quantifies the imbalance between right- and left-handed quarks. The resulting final-state charge separation, termed the chiral magnetic effect (CME) [1], is of great experimental and theoretical interest. However, its experimental characterization has been hampered by significant background.

The charge separation can be quantified via the  $P$ -odd sine term  $a_1$ , in the Fourier decomposition of the charged-particle azimuthal distribution [3]:

$$\frac{dN_{\text{ch}}}{d\phi} \propto 1 + 2 \sum_n (v_n \cos(n\Delta\phi) + a_n \sin(n\Delta\phi) + \dots) \quad (1)$$

where  $\Delta\phi = \phi - \Psi_{\text{RP}}$  gives the particle azimuthal angle with respect to the reaction plane (RP) angle, and  $v_n$  and  $a_n$  denote the coefficients of the  $P$ -even and  $P$ -odd Fourier terms, respectively. A direct measurement of  $a_1$ , is not possible due to the strict global  $\mathcal{P}$  and  $\mathcal{CP}$  symmetry of QCD. However, their fluctuation and/or variance  $\tilde{a}_1 = \langle a_1^2 \rangle^{1/2}$  can be measured with charge-sensitive correlators such as the  $\gamma$ -correlator [3] and the  $R_{\Psi_2}(\Delta S)$  correlator [4].

The  $\gamma$ -correlator measures charge separation as:  $\gamma_{\alpha\beta} = \langle \cos(\phi_\alpha + \phi_\beta - 2\Psi_2) \rangle$ ,  $\Delta\gamma = \gamma_{0S} - \gamma_{SS}$ , where  $\Psi_2$  is the azimuthal angle of the 2<sup>nd</sup>-order event plane which fluctuates

\*e-mail: Roy.Lacey@Stonybrook.edu

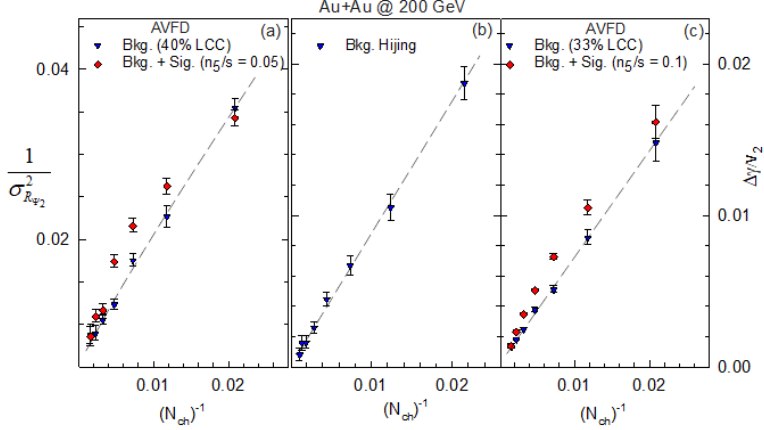


**Figure 1.**  $\sigma_{R_{\Psi_2}}^{-2}$  vs.  $1/N_{\text{ch}}$  (a) and  $\Delta\gamma/v_2$  vs.  $1/N_{\text{ch}}$  (b) and (c) for simulated Au+Au collisions at  $\sqrt{s_{\text{NN}}} = 200$  GeV. The results for  $\sigma_{R_{\Psi_2}}^{-2}$  and  $\Delta\gamma/v_2$  from the AVFD model are shown for background and for signal + background as indicated. The Hijing model results are only shown for the background. The dashed lines represent linear fits to the background values.

about the RP,  $\phi$  denote the particle azimuthal emission angles,  $\alpha, \beta$  denote the electric charge (+) or (-) and SS and OS represent same-sign (++, --) and opposite-sign (+-) charges. Measurements of the quotient  $\Delta\gamma/v_2$  with the 2<sup>nd</sup>-order anisotropy coefficient  $v_2$ , are usually employed to aid quantification of the background-driven charge separation.

The  $R_{\Psi_2}(\Delta S)$  correlator measures charge separation relative to  $\Psi_2$  via the ratio:  $R_{\Psi_2}(\Delta S) = C_{\Psi_2}(\Delta S)/C_{\Psi_2}^{\perp}(\Delta S)$ , where  $C_{\Psi_2}(\Delta S)$  and  $C_{\Psi_2}^{\perp}(\Delta S)$  are correlation functions that quantify charge separation  $\Delta S$ , approximately parallel and perpendicular (respectively) to the  $\vec{B}$ -field. The charge-shuffling procedure used to construct the correlation functions ensures identical properties for their numerator and denominator, except for the charge-dependent correlations, which are of interest [4].  $C_{\Psi_2}(\Delta S)$  measures both CME- and background-driven charge separation while  $C_{\Psi_2}^{\perp}(\Delta S)$  measures only the background. After correcting the  $R_{\Psi_2}(\Delta S)$  distributions for the effects of particle-number fluctuations and the event-plane resolution, their inverse variance  $\sigma_{R_{\Psi_2}}^{-2}$  are used to quantify the charge separation [4].

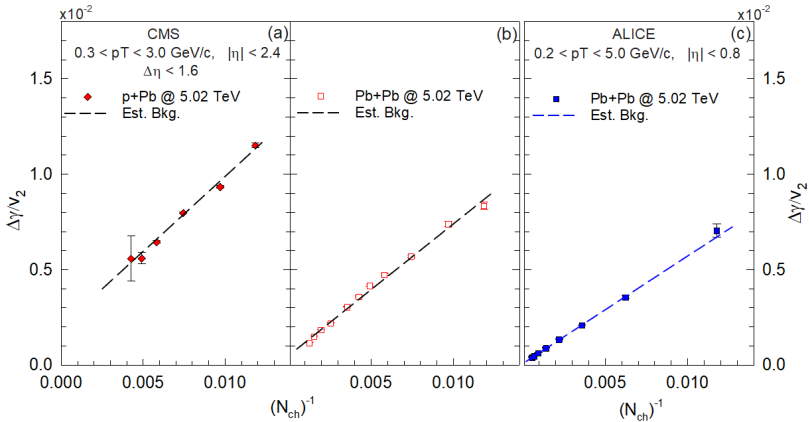
In this work, we use model simulations to chart the scaling properties of  $\sigma_{R_{\Psi_2}}^{-2}$  and  $\Delta\gamma/v_2$  for the background and signal + background, respectively, in A+A collisions. We then leverage these scaling properties to identify and characterize a possible CME-driven charge separation using previously published data for  $p$ +Au,  $d$ +Au, Ru+Ru, Zr+Zr and Au+Au collisions at RHIC [5–10], and  $p$ +Pb and Pb+Pb collisions at the LHC [11–14].

Figure 1 shows the results for  $\sigma_{R_{\Psi_2}}^{-2}$  and  $\Delta\gamma/v_2$  obtained with the AVFD and Hijing models for Au+Au collisions. Note that these models emphasize different sources for the charge-dependent non-flow background. The AVFD model also allows input values for the initial axial charge density  $n_5/s$  and the degree of local charge conservation (LCC) that regulate the magnitude of the CME- and background-driven charge separation. The solid triangles in Fig. 1 show that the background [for both models] scales as  $1/N_{\text{ch}}$  – the expected trend for the charge-dependent non-flow correlations. By contrast, the signal (Sig.) + background values (solid diamonds) indicate positive deviations from the background scaling [16, 17]. This dependence can be represented as;  $\Delta\gamma/v_2 = a + b/(N_{\text{ch}})^{1-c}$ , and  $\sigma_{R_{\Psi_2}}^{-2} = a' + b'/(N_{\text{ch}})^{1-c'}$ , for the small values of  $n_5/s$  indicated in Fig. 1. Here,  $a, b$  and  $c$  are parameters;  $c$  characterizes

the degree of the scaling violation and the magnitude of the CME; for  $c \sim 0$  the  $1/N_{\text{ch}}$  scaling for the background is retrieved, as demonstrated for  $\sigma_{R\psi_2}^{-2}$  and  $\Delta\gamma/v_2$  with the AVFD model in Fig. 1.

The scaling violation for  $\sigma_{R\psi_2}^{-2}$  and  $\Delta\gamma/v_2$  (Figs. 1 (a) and (c)) gives a direct signature of the CME-driven contributions to the charge separation. It can be quantified via  $c > 0$  and the fractions:  $f_{\text{CME}}^{\Delta\gamma} = [\Delta\gamma/v_2(\text{Sig.} + \text{Bkg.}) - \Delta\gamma/v_2(\text{Bkg.})]/[\Delta\gamma/v_2(\text{Sig.} + \text{Bkg.})]$ ,  $f_{\text{CME}}^R = [\sigma_{R\psi_2}^{-2}(\text{Sig.} + \text{Bkg.}) - \sigma_{R\psi_2}^{-2}(\text{Bkg.})]/[\sigma_{R\psi_2}^{-2}(\text{Sig.} + \text{Bkg.})]$ . The scaling patterns in Fig. 1 suggest that the observation of  $1/N_{\text{ch}}$  scaling for the experimental  $\sigma_{R\psi_2}^{-2}$  and  $\Delta\gamma/v_2$  measurements would strongly indicate background-driven charge separation with little room for a CME contribution. However, observing a violation of this  $1/N_{\text{ch}}$  scaling would indicate the CME-driven contribution. Figs. 1 (a) and (c) also indicate comparable background and signal + background  $\sigma_{R\psi_2}^{-2}$  and  $\Delta\gamma/v_2$  values in central and peripheral collisions, suggesting that the background dominates over that of the CME-driven contributions in these collisions. This trend for the background is consistent with the reduction of  $\vec{B}$  in central collisions and the enhanced de-correlation between the event plane and the  $\vec{B}$ -field in peripheral collisions.

Since the background dominates in central and peripheral collisions, the  $\sigma_{R\psi_2}^{-2}$  and  $\Delta\gamma/v_2$  measurements for these collisions can be leveraged with  $1/N_{\text{ch}}$  scaling to obtain a quantitative estimate of the background over the entire centrality span (cf. Fig. 1). Here, an important proviso is to experimentally establish that the background in  $p(d)+A$  and  $A+A$  collisions scale as  $1/N_{\text{ch}}$  over the full centrality span.



**Figure 2.**  $\Delta\gamma/v_2$  vs.  $1/N_{\text{ch}}$  for  $p+Pb$  (a) and  $Pb+Pb$  [(c) and (d)] collisions at  $\sqrt{s_{\text{NN}}} = 5.02$  TeV. The dashed lines indicate an estimate of the background. The data are taken from Refs. [12, 13, 15].

The  $v_2$  and  $\Delta\gamma$  values reported for  $p+Au$ ,  $d+Au$ ,  $Ru+Ru$ ,  $Zr+Zr$  and  $Au+Au$  collisions at RHIC [5–10], and  $p+Pb$  and  $Pb+Pb$  collisions at the LHC [12–15] were used to investigate the scaling properties of  $\Delta\gamma/v_2$ . Fig. 2 shows the results for  $p+Pb$  and  $Pb+Pb$  collisions at  $\sqrt{s_{\text{NN}}} = 5.02$  TeV. They indicate that  $\Delta\gamma/v_2$  essentially scales as  $1/N_{\text{ch}}$  ( $c \approx 0$ ), suggesting negligible CME contributions in these collisions. They also confirm that the combined sources of background (LCC, resonances, back-to-back jets, ...), which should be substantial, especially for  $p+Pb$ , scale as  $1/N_{\text{ch}}$ . Note as well that the CME contribution is negligible in  $p(d)+A$  collisions because of significant reductions in  $\vec{B}$ , and the sizable de-correlation between the event plane and the  $\vec{B}$ -field [12]. Thus, the scaling patterns of  $\Delta\gamma/v_2$  for these

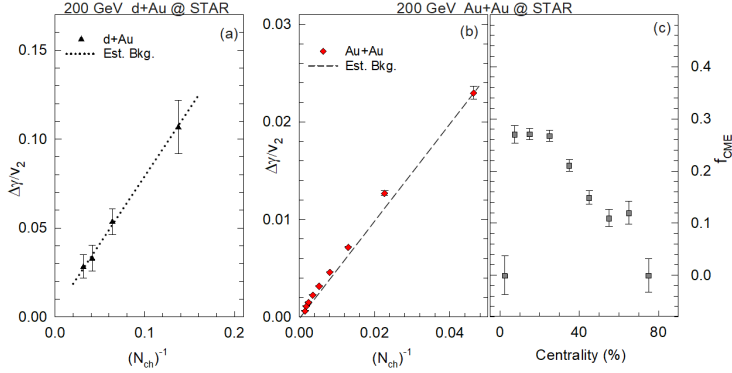


**Figure 3.**  $\Delta\gamma/v_2$  vs.  $1/N_{\text{ch}}$  [(a) and (b)] and  $f_{\text{CME}}$  vs. centrality (c) for  $d+\text{Au}$  and  $\text{Au}+\text{Au}$  collisions at  $\sqrt{s_{\text{NN}}} = 200$  GeV. The dotted and dashed lines indicate an estimate of the background contributions. The data are taken from Refs. [7, 9? ].

systems' sizable backgrounds give a direct experimental constraint on the validity of  $1/N_{\text{ch}}$  scaling of the background.

The scaling results for collisions at  $\sqrt{s_{\text{NN}}} = 200$  GeV are shown in Fig. 3. The  $1/N_{\text{ch}}$  scaling apparent for  $d+\text{Au}$  collisions (Fig. 3 (a)) confirms the expectation that the CME is negligible in these collisions. It also confirms that the combined sources of background (LCC, resonances, back-to-back jets, ...), which could be substantial in  $d+\text{Au}$  collisions, show  $1/N_{\text{ch}}$  scaling. In contrast to  $d+\text{Au}$ , the results for  $\text{Au}+\text{Au}$  (Fig. 3(b)) show visible indications of a violation ( $c > 0$ ) to the  $1/N_{\text{ch}}$  scaling observed for background-driven charge separation in  $p(d)+\text{A}$  collisions. Similar violations were observed for  $\text{Ru}+\text{Ru}$  and  $\text{Zr}+\text{Zr}$  [17]. The scaling violation is similar to that observed for signal + background in Figs. 1 (a) and (c), suggesting an unambiguous non-negligible CME contribution to the measured  $\Delta\gamma/v_2$  in  $\text{Au}+\text{Au}$ ,  $\text{Ru}+\text{Ru}$ , and  $\text{Zr}+\text{Zr}$  collisions. The CME contribution can be quantified via fits with the function  $\Delta\gamma/v_2 = a + b/(N_{\text{ch}})^{1-c}$ , to evaluate  $c$ . Alternatively, estimates of the background for all three systems can be estimated by leveraging the  $\Delta\gamma/v_2$  measurements for peripheral and central collisions with  $1/N_{\text{ch}}$  scaling [17]. Here, it is important to recall that the simulated results from the AVFD and HIJING models, as well as the measurements presented in Figs. 2 and 3(a), provide strong constraints that the combined sources of background, scale as  $1/N_{\text{ch}}$  over the full centrality span. The background estimates were used to extract  $f_{\text{CME}}$  values for  $\text{Au}+\text{Au}$ , (Fig. 3 (c))  $\text{Ru}+\text{Ru}$  and  $\text{Zr}+\text{Zr}$  collisions respectively. They indicate non-negligible  $f_{\text{CME}}$  values that vary with centrality. In mid-central collisions,  $f_{\text{CME}} \sim 27\%$  for  $\text{Au}+\text{Au}$  collisions, which is roughly a factor of two larger than the values for  $\text{Ru}+\text{Ru}$  and  $\text{Zr}+\text{Zr}$ . Within the uncertainties, no significant difference between the values for  $\text{Ru}+\text{Ru}$  and  $\text{Zr}+\text{Zr}$  was observed, suggesting that  $\Delta\gamma/v_2$  is sensitive to CME-driven charge separation in  $\text{Ru}+\text{Ru}$  and  $\text{Zr}+\text{Zr}$  collisions but may be insensitive to the signal difference between them [17].

In summary, we demonstrate that the scaling properties of the  $R_{\Psi_2}(\Delta S)$  and the  $\Delta\gamma$  correlators can be used to characterize the CME in colliding systems at RHIC and the LHC. The  $\Delta\gamma/v_2$  measurements for  $p+\text{Au}$  and  $d+\text{Au}$  collisions at  $\sqrt{s_{\text{NN}}} = 200$  GeV and  $p+\text{Pb}$  ( $\sqrt{s_{\text{NN}}} = 5.02$  TeV) and  $\text{Pb}+\text{Pb}$  collisions at  $\sqrt{s_{\text{NN}}} = 5.02$  and 2.76 TeV, scales as  $1/N_{\text{ch}}$  consistent with background-driven charge separation. However, the results for  $\text{Au}+\text{Au}$ ,  $\text{Ru}+\text{Ru}$  and  $\text{Zr}+\text{Zr}$  collisions ( $\sqrt{s_{\text{NN}}} = 200$  GeV) show scaling violations, which indicate a CME-driven contribution in the presence of significant background. In mid-central collisions,

$f_{\text{CME}} \sim 27\%$  for Au+Au collisions and is approximately a factor of two smaller in Ru+Ru and Zr+Zr collisions with similar magnitudes for the two isobars.

## References

- [1] D. Kharzeev, Phys. Lett. B **633**, 260-264 (2006)
- [2] M. Asakawa, A. Majumder and B. Muller, Phys. Rev. C **81** (2010), 064912
- [3] S. A. Voloshin, Phys. Rev. C **70** (2004), 057901
- [4] N. Magdy *et al.*, Phys. Rev. C **97** (2018) no.6, 061901
- [5] B. I. Abelev *et al.* [STAR], Phys. Rev. C **81** (2010), 054908
- [6] B. I. Abelev *et al.* [STAR], Phys. Rev. Lett. **103** (2009), 251601
- [7] L. Adamczyk *et al.* [STAR], Phys. Rev. C **88** (2013) no.6, 064911
- [8] L. Adamczyk *et al.* [STAR], Phys. Rev. Lett. **113** (2014), 052302
- [9] J. Adam *et al.* [STAR], Phys. Lett. B **798** (2019), 134975
- [10] M. Abdallah *et al.* [STAR], Phys. Rev. C **105** (2022) no.1, 014901
- [11] B. Abelev *et al.* [ALICE], Phys. Rev. Lett. **110** (2013) no.1, 012301
- [12] V. Khachatryan *et al.* [CMS], Phys. Rev. Lett. **118** (2017) no.12, 122301
- [13] A. M. Sirunyan *et al.* [CMS], Phys. Rev. C **97** (2018) no.4, 044912
- [14] S. Acharya *et al.* [ALICE], Phys. Lett. B **777** (2018), 151-162
- [15] S. Acharya *et al.* [ALICE], JHEP **09** (2020), 160
- [16] R. A. Lacey, N. Magdy, P. Parfenov and A. Taranenko, [arXiv:2203.10029 [nucl-ex]].
- [17] R. A. Lacey and N. Magdy, [arXiv:2206.05773 [nucl-ex]].